

PCCP

Accepted Manuscript



This is an *Accepted Manuscript*, which has been through the Royal Society of Chemistry peer review process and has been accepted for publication.

Accepted Manuscripts are published online shortly after acceptance, before technical editing, formatting and proof reading. Using this free service, authors can make their results available to the community, in citable form, before we publish the edited article. We will replace this *Accepted Manuscript* with the edited and formatted *Advance Article* as soon as it is available.

You can find more information about *Accepted Manuscripts* in the [Information for Authors](#).

Please note that technical editing may introduce minor changes to the text and/or graphics, which may alter content. The journal's standard [Terms & Conditions](#) and the [Ethical guidelines](#) still apply. In no event shall the Royal Society of Chemistry be held responsible for any errors or omissions in this *Accepted Manuscript* or any consequences arising from the use of any information it contains.

Laboratory Astrochemistry: Catalytic Conversion of Acetylene to Polycyclic Aromatic Hydrocarbons over SiC Grains

T.Q. Zhao^a, Q. Li^a, B.S. Liu^{ab*}, R.K.E. Gover^c, P.J. Sarre^c and A. S.-C. Cheung^{a*}

^a Department of Chemistry, The University of Hong Kong, Pokfulam Road, Hong Kong, China,

^b Department of Chemistry, Tianjin university, and Collaborative Innovation Center of Chemical Science and Engineering (Tianjin), Tianjin 300072, China,

^c School of Chemistry, The University of Nottingham, University Park, Nottingham NG7 2RD, UK

Text : 23

Scheme : 1

Table : 1

Figures : 7

Corresponding Author, E-mail: hrscsc@hku.hk, Phone 00852-28582155

* Corresponding Author, E-mail: hrscsc@hku.hk, Phone 00852-28582155, bingliliu@tju.edu.cn

Abstract

Catalytic conversion reactions of acetylene on a solid SiC grain surface lead to the formation of polycyclic aromatic hydrocarbons (PAHs) and are expected to mimic chemical processes in certain astrophysical environments. Gas-phase PAHs and intermediates were detected *in situ* using time-of-flight mass spectrometry, and their formation was confirmed using GC-MS in a separate experiment by flowing acetylene gas through a fixed-bed reactor. Activation of acetylene correlated closely with the dangling bonds on the SiC surface which interact with and break the C-C π bond. Addition of acetylene to the resulting radical site forms a surface ring structure which desorbs from the surface. The results of HRTEM and TG indicate that soot and graphene formation on the SiC surface depends strongly on reaction temperature. We propose that PAHs as seen through the 'UIR' emission bands can be formed through decomposition of graphene-like material, formed on the surface of SiC grains in carbon-rich circumstellar envelopes.

Keywords: Polycyclic aromatic hydrocarbon molecule; Dangling bonds; Nano-SiC grains; Time-of-flight mass spectrometry; Astrochemistry; Mechanism

Introduction

During the last four decades, abundant and ubiquitous PAHs have been discovered in very many types of astrophysical object and environments, including H II regions, reflection nebulae, young stellar objects, planetary nebulae (PNe), asymptotic giant branch (AGB) objects, the nuclei of galaxies and ultraluminous infrared galaxies (ULIRGs)¹, through a set of so-called ‘unidentified’ infrared (UIR, *i.e.* 3.3, 6.2, 7.7, 8.6 and 11.2 μm) emission bands for which PAHs are held responsible^{2,3}. PAHs play an important role in astrochemistry¹, and the formation chemistry of PAHs is widely discussed.^{4,5} From a chemical point of view, PAHs can be formed by aromatization of acetylene, which is an abundant molecule in carbon-rich circumstellar envelopes (CSEs)^{6,7}. However, a complete mechanism for cosmic PAH formation is still lacking or disputed. Cherchneff⁸, Frenklach *et al.*⁹ and Cole *et al.*¹⁰ have proposed radical-based mechanisms that involve acetylene, whereas Woods *et al.*¹¹ and Carelli *et al.*¹² favour PAH formation through ion-molecule reactions. Based on laboratory studies, a Lewis acid catalytic mechanism involving reactions of acetylene over silicates, as would be present in mixed-chemistry astrophysical environments, has been put advanced.^{13, 14} We report here an acetylene activation mechanism involving dangling bonds on SiC surfaces which leads to the formation of aromatic molecules and a surface graphene-like coating.

Solid SiC is a major component of the dust in the circumstellar envelopes of mass-losing carbon-rich stars and is found in pre-solar meteorites and in comet material returned to Earth by the Stardust mission.¹⁵ A overview of SiC grains in astrophysical

environments is given by Speck *et al.*¹⁶ and for meteorites and interplanetary dust particles by Hoppe.¹⁷ SiC in carbon-rich objects is identified principally through its characteristic infrared emission band at $\sim 11 \mu\text{m}$, which in a few objects is seen in absorption. Based on comparison of astronomical spectra with laboratory and meteorite sample spectroscopic data, the observed $\sim 11 \mu\text{m}$ feature is attributed to β -SiC.^{18,19} There is no clear evidence for SiC in the interstellar medium possibly due to oxidation of the particles,²⁰ but it has recently been identified in the proto-planetary disc¹⁵ of the pre-main-sequence object SVS13. Recently, Merino *et al.*²¹ proposed that SiC grains play a role in the formation of PAHs through a ‘top-down mechanism’, where graphene is formed on a single crystal 6H-SiC(0001) surface as a consequence of annealing the SiC at $1227 \text{ }^\circ\text{C}$. The graphene layer (at about $927 \text{ }^\circ\text{C}$) was then etched by H atoms which induced surface modifications which are thought to yield PAH fragments, although these were not detected in the experiments undertaken. In this scenario PAHs are released to the gas phase within the CSE beyond *c.* 5 stellar radii but not into the general ISM.

Silicon carbide (SiC) is an important material which shows great potential for high-power devices²² due to its high thermal conductivity, high electric field breakdown strength and high maximum current density. SiC is not generally known to be a catalytic material, but the large surface area and high chemical inertness of β -SiC makes it a valuable catalyst support²³, which has been applied in a variety of heterogeneous catalysis reactions. Sun *et al.*²⁴ have reported the partial oxidation of methane over a Ni/SiC catalyst and Church *et al.*²⁵ have studied cellulose conversion

to hydrogen using a similar catalyst. In addition, nanodiamonds/ β -SiC composite as metal-free catalysts was used for steam-free dehydrogenation of ethylbenzene to styrene²⁶. SiC is composed solely of silicon and carbon, each atom being bonded to four atoms of the other element. At the crystal surface, the unsatisfied valence tends to be compensated for by surface relaxation which significantly reduces the spacing distance between the surface layer and the layer just below it, and brings about surface reconstruction – a more substantial rearrangement of the atoms that reforms the crystal structure at the surface in order to reduce the number of dangling bonds²⁷. A silicon dangling bond, sometimes referred to as a silicon radical, has a single unpaired electron. Its chemisorption ability makes it possible for the silicon dangling bond to act as an active site for certain chemical reactions. However, to the best of our knowledge, aromatization of small molecules such as acetylene on SiC has not been reported previously. The presence of acetylene in carbon-rich CSEs is well established. In order to understand better the formation of PAHs in circumstellar environments, this research is conducted in a hypothetical-deductive model of reasoning. The coexistence of acetylene, PAHs and SiC grains in astrophysical environments suggests that there could be a connection between them. It is hypothesized here that SiC has a catalytic effect on acetylene aromatization, and this hypothesis is supported by experiments which show that acetylene aromatization over SiC produces PAHs.

Experimental

Physical properties of samples and characterization

The reagent gases used in our experiments including acetylene (99%), propyne, 2-butyne, propylene, ethylene and propane were purchased directly from chemical companies. Solid SiC has two crystalline forms, α -SiC and β -SiC, which were directly purchased from Alfa Aesar (α -SiC: 99.8%, particle size of 2 μm , 9-11 m^2/g) and (β -SiC: 99.8%, particle size of 1 μm , 11.5 m^2/g) and used without further treatment. Our EDX analysis indicated that no measurable amounts of metal elements were present, i.e. both α -SiC and β -SiC samples have no measurable amount of metal elements. The certificates of analysis provided by the Alfa Aesar company showed that trace amounts of aluminum, calcium and iron were present as impurities; they are lower than the 0.03% level which is consistent with our EDX results.

Powder XRD patterns of clean SiC were recorded using a Bruker AXS D8 Advance powder X-ray diffractometer with Cu K α monochromatic radiation ($\lambda = 0.15406 \text{ nm}$, 40 kV, 40 mA). High resolution transmission electron microscopy (HR-TEM) of SiC was conducted on a Tecnai G2 F20 electron microscope at 200 kV accelerating voltage. Fourier Transform Infrared (FT-IR) spectra of α -SiC and β -SiC were acquired on an FT-IR 8300 spectrophotometer (Shimadzu). TG/DTG analysis of used SiC was conducted in air (20-25 mL/min) on a NETZSCH STA 409 PC/PG thermogravimetric analyzer. Approximately 2-3 mg sample was heated from room temperature to 100 $^{\circ}\text{C}$ and maintained at this temperature for 5 min before being heated up to 750 $^{\circ}\text{C}$ at a rate of 10 $^{\circ}\text{C}/\text{min}$.

Apparatus and experimental condition

A schematic of the time-of-flight mass-spectrometer (TOF-MS) used for these studies is shown in Fig. 1. This homebuilt instrument consists of a source chamber with a quartz tube fixed-bed reactor, an ionization chamber, a TOF tube and a detection chamber. The feeding device was connected to the reactor and reactant gas was introduced *via* an electronically-controlled pulsed valve (diameter: 0.15 mm; backing pressure: 3 bar). A skimmer with a 2 mm diameter aperture was used to separate the source chamber (3×10^{-6} Torr) and ionization chamber (2×10^{-6} Torr). A two-stage TOF lens assembly (including source backing plate, ionization and acceleration region) and an ion-beam focusing Einzel lens setup were located inside the ionization chamber, where the ionization of gaseous species was achieved through multi-photon processes. The detection chamber was connected to the TOF tube and a multi-channel plate (MCP) detector was used to detect the arrival of ions. For each experiment, about 100 mg of α - or β -SiC catalyst was placed inside the quartz tube reactor. After the SiC was pretreated to 600 °C with flowing argon, the reagent gas was sent in pulsed mode to the reactor at a repetition rate of 10 Hz and with pulse duration of 250-300 μ s. Catalytic aromatization reactions occurred in the temperature range 400 to 750 °C. The products of the reaction were injected directly into the ionization chamber through the skimmer, and ionized by an ArF excimer laser (193 nm; 10 Hz repetition; 8-9 mJ and pulse width of 8 ns) to generate molecular ions, which were accelerated by high voltage and travelled through the standard TOF field-free region. The signals recorded by the MCP detector were forwarded to a 300 MHz oscilloscope for averaging.

In a separate experiment using a continuous flow of acetylene gas at atmospheric pressure over the SiC catalyst, the obtained products were analyzed using gas chromatography-mass spectrometry (GC-MS). This experiment was undertaken to investigate the larger PAHs adsorbed on the SiC surface, and as our home-built TOF-MS has relatively low mass resolution (limited to only unit mass). The higher mass accuracy (up to 0.05 mass unit) from the GC-MS experiments confirmed the masses of individual molecular species and, more importantly, each MS fragment pattern is unique for an individual molecule, which confirmed unambiguously the structure of the carrier of a compound of specific mass. In addition, we noticed that the heavier PAHs formed (i.e. those with mass larger than 250) likely condense on the surface of the catalyst, and so their presence might not be detectable using the TOF-MS technique. The GC-MS study therefore provided important information on high mass PAH species in this work. In this experiment, a quartz tube reactor was housed in a furnace and about 100 mg of SiC was placed inside the quartz tube. After the catalyst was pretreated in argon, acetylene gas was allowed to flow for 30 minutes, and the effluent gas after passing through the SiC catalyst was directed to go through a cold trap to condense volatile compounds. In addition, there were also PAHs deposited on the SiC surface. These solids were analyzed using GC-MS.

Results and discussion

Structure and properties of SiC

The HRTEM images of α -SiC (Fig. 2a) exhibit an ordered morphology of

hexagonal crystal structure and its selected area electron diffraction (SAED) pattern (inset in Fig. 2a) reveals that the distances between the two bright spots are 0.270 nm and 0.252 nm, corresponding to the diffraction of the (101) and (102) lattice planes of 6H-SiC. In addition, a zinc blende cubic structure was observed for β -SiC (Fig. 2b) and the SAED pattern of β -SiC presented a dispersive circle mode; this illustrates the existence of multicrystallites of nano-SiC grains, and the four rings with spots in SAED pattern that can be indexed (from inner to outer) to (111), (200), (220), and (311) planes of β -SiC (inset of Fig. 2b). The XRD patterns of α -SiC and β -SiC are shown in Fig. 2c; it can be seen that that β -SiC presents a 3C-SiC structure (PDF 29-1129) and α -SiC has the structure of 6H-SiC (PDF: 29-1128) with a small amount of 4H-SiC (PDF: 29-1127) similar to that observed in Murchison meteorite.²¹ As shown in Fig. 2d, there is a broad absorption band due to the Si-C stretching vibration at 11.3 μm and a very weak shoulder peak at 12.7 μm , resulting from the longitudinal optic (LO) branch resonance of β -SiC²⁸ in the FT-IR spectrum of β -SiC. In contrast, the FT-IR spectrum of α -SiC has a strong vibrational stretching band of Si-C at 11.9 μm and a weak shoulder at 10.7 μm that are consistent with excitation of the transverse optic (TO) branch of α -SiC.²⁹

Acetylene conversion reactions for forming PAHs over β -SiC (or α -SiC) were investigated in the temperature range of 400-750 °C. The products detected by time-of-flight mass spectrometry (TOF-MS) (Fig. 3) indicate that when the temperature was higher than 400 °C, PAHs such as naphthalene, anthracene/phenanthrene, pyrene etc were formed and reached a maximum at 600 °C. However, there was a noticeable

difference in the production of a few compounds and in particular naphthalene ($m = 128$), anthracene /phenanthrene ($m = 178$) and pyrene ($m = 202$) tended to be produced more readily at higher temperature. In order to be certain that the PAHs produced originated from the catalytic reaction rather than from reaction with any materials or the surface of the quartz tube in the oven, we performed a control experiment. In this experiment, when acetylene was pulsed into the quartz reaction tube with no SiC present, no PAHs were formed. It was found experimentally for the first time that the reaction of acetylene aromatization occurred on SiC leading to the formation of PAHs. Similar results were obtained from the atmospheric pressure continuous flow experiment, in which, besides condensing the volatile products from the effluent gas, PAH material was also found to be deposited on the SiC surface. Both of the solid samples collected were dissolved in dichloromethane (DCM). For ease of reference, the solution obtained from dissolving the deposits on the SiC surface and from the cold trap are named Solution A and Solution B, respectively. The solutions were analyzed using gas chromatography mass spectrometry (GC-MS) with a flame ionization detector and the results are shown in Fig. 4.

The PAHs formed were the same as those in the TOF-MS experiments. However, it is interesting to note that the GC-MS spectrum of Solution A showed a dramatic increase in larger PAHs such as acenaphthylene, phenanthrene, anthracene, pyrene, chrysene and dibenz[a,h]anthracene compared with Solution B. This is probably due to the fact that smaller PAHs could be readily desorbed from the SiC surface whereas heavier PAHs tended to remain on the surface.

Figure 5 shows the formation of PAHs over α -SiC and β -SiC, respectively. It can be seen that the catalytic activity of β -SiC was significantly higher in producing PAHs than α -SiC at low temperature (≤ 600 °C), indicating that lower temperature is more favourable for β -SiC due to a structure of dispersive multi-crystallites (Fig. 2b). At about 650 °C, both forms of SiC yielded similar PAHs. According to the report of Shukla *et al.*³⁰, the formation of benzene and phenylacetylene from acetylene in the gas phase can only occur at 1001 °C with no catalyst present. This indicates that solid SiC grains can reduce the conversion temperature significantly for the formation of PAHs from acetylene. Such conditions would be favourable for the conversion of acetylene to PAHs in circumstellar envelopes (CSEs). In our experiments, we also observed catalytic deactivation after about 10 minutes and the production of PAHs began to decrease; this deactivation occurred when the active sites became covered with hydrogenated and amorphous carbon.³¹

Graphene formed on the surface of silicon carbide

As presented in Fig. 6, thermogravimetric analysis (TG) on α -SiC and β -SiC, after reaction, showed that significant weight loss occurred at 550–680 °C on used α -SiC whereas the temperature range for weight loss was 500–620 °C over used β -SiC, and the weight loss (amount of carbon deposition on the surface) increased with an increase in reaction temperature (Fig. 6a-b). This explains the deactivation of SiC at high temperature³² because the pure SiC gained extra mass (the upper line in Fig. 6a-b). The high-resolution transmission electron microscopy (HRTEM) images (Fig. 6c-d) of the used SiC also showed the existence of a clear graphene structure or parallel

graphitic layers stacked on the surface of SiC.

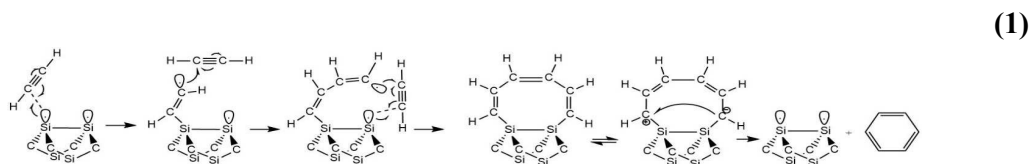
In fact, the ability to form graphitic structures gives further support for acetylene aromatization reactions over SiC as a catalyst. However, the formation of graphitic layers here did not result from annealing³³ of SiC because graphene formation on SiC by annealing was shown to be a temperature higher than 1250 °C by Merino *et al*²¹ and neither graphene nor graphite was observed on the SiC surface when heated to 750 °C without acetylene. Therefore, the formation of PAHs reported here must follow other mechanism.

Various kinds of carbon deposition on catalytic surfaces have been studied in detail in the fields of industrial heterogeneous catalysis^{34, 32} and carbon stability in geochemistry.³⁵ Carbon deposits can be oxidized at various temperatures. Hydrogenated carbon³² is the most active species that can be oxidized below 300 °C; graphitic carbon or carbon nanotubes can be removed at around 420 °C, while carbon black has the highest thermal stability and can hardly be removed below 600 °C. Our TG/DTG result reveals that carbon species deposited on SiC after acetylene reaction contributed to the formation of graphene or graphitic carbon black on the surface.

Mechanism of PAHs formed on dangling bonds of SiC

For acetylene catalytic aromatization reactions on an SiC surface, the dangling bonds on the SiC surface are potential active sites for chemisorption and activation. As described in **Process 1**, an acetylene molecule adsorbs on a silicon dangling bond to generate a silylacetylenyl radical, which then bonds with another acetylene molecule

to generate a 1-buten-3-ynyl radical. After another acetylene molecule bonds with the diene, the carbon radical attacks another Si dangling bond to form an octatomic ring, which has an unstable resonance structure with a positive and a negative charge at each end of the triene due to a triene conjugation entity.



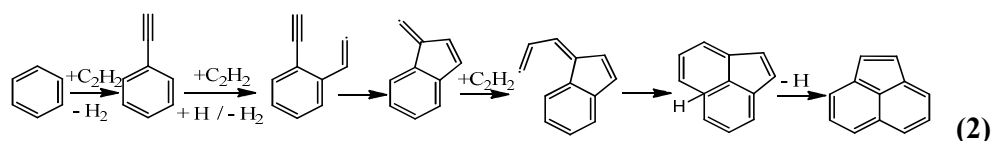
Based on density functional theory (DFT) calculation results and the exchange-correlation functional according to Perdew and Wang³⁶, there is an on-top (OT) site in which an acetylene molecule is di- σ bonded to a top layer Si dimer (silicon dangling bond) with the molecular C-C axis parallel to the dimer direction. From the calculation, which yields an adsorption energy of 2.56 eV in the local density approximation (or 3.22 eV in the generalized gradient approximation)³⁷, it is clear that the OT sites are occupied rapidly upon acetylene exposure. This further confirms our proposed reaction mechanism. Moreover, as stated above, the Si-Si dimer on the reconstructed surface of a SiC(001) has a bond distance of 2.73 Å and the Si-Si bond is therefore very weak. Hence it is highly plausible that the octatomic ring undergoes a rearrangement process to form a benzene ring in order to achieve the most stable structure.

In order to study further the mechanism of acetylene aromatization on dangling bonds of SiC, a series of hydrocarbons, including acetylene, propyne, 2-butyne, ethylene, propylene and propane were used to investigate the process of experimental

PAH formation on SiC. As shown in Fig. 7, the amount of PAH formation is closely related to the type of C-C bond and the presence of substituted groups. The PAH signals formed from acetylene over SiC were markedly higher than those from propyne and 2-butyne due to the fact that the C≡C triple bond connected to hydrogen is more likely to attack the dangling bonds on β-SiC(001). Thus, the 2-butyne aromatization over SiC exhibited weaker signals due to steric hindrance of the methyl groups. In addition, the efficiency of the aromatic reaction involving ethene and propylene on the dangling bonds of β-SiC(001) was significantly lower (Fig. 7) because the double bond in the alkene interacts with a Si dangling bond to become chemisorbed on the SiC surface, and the carbon atom in the alkene undergoes a conversion³⁸ from sp² to sp³ hybridization. DFT calculations also confirmed that the adsorption energy of ethylene (3.07 eV) is lower than that of acetylene (3.22 eV) on the dangling bond of SiC³⁷, so the signal of PAHs reduced substantially and there was no observable signal generation for propane as reactant. In summary, the C≡C triple bond is the most reactive with the Si dangling bond, the C=C double bond less so, with the least reactive being the C–C single bond.

As discussed earlier, the formation of the initial benzene ring is the crucial rate-determining step for the PAH formation. After the closure of the first aromatic ring, larger PAHs are formed following various routes according to the H-abstraction/C₂H₂ addition (HACA) mechanism. In order to have a clear understanding of the pathways, PAHs and intermediates with the same mass intervals are grouped together (Table 1) which was in the map for acetylene aromatization (**Scheme 1**).

Following the formation of benzene, the first mass number sequence of 24 appear at $m = 78, 102, 126$ and 150 as a consequence of acetylene addition¹³. The second sequence with a mass interval of 50 is observed at $m = 128, 178, 228$ based on the addition of diacetylene. PAHs ($m = 252, 276$) are formed starting from triphenylene ($m = 228$) by adding acetylene in the bay hydrogen sites. In addition, pyrene ($m = 202$) can be formed by addition of acetylene to phenanthrene ($m = 178$) and the dimerization of pyrene occurred at low temperature to produce the soot particle size distribution³⁹. In **Scheme 1**, acenaphthalene ($m = 152$) and pyracylene ($m = 176$) can be generated by adding acetylene to naphthalene ($m = 128$) while abstracting hydrogen. However, according to Kislov *et al.*⁴⁰ (**Process 2**), the yield of acenaphthalene ($m = 152$) is much higher than that by the pathway in **Scheme 1**.



It should not be neglected that PAHs with an odd number of carbon atoms are formed in the acetylene conversion, such as the indenyl radical ($m = 115$), indenylacetylene ($m = 139$), the fluorenyl radical ($m = 165$), fluorenylacetylene ($m = 189$) and the fluorenyldiethynyl radical ($m = 213$). The propargyl radical reacted with benzene to form an indenyl radical (Fig. 3, 600 °C); a similar mechanism at high temperature (927- 1227 °C) was reported by Zhang *et al.*⁴¹. As shown in **Scheme 1**, starting from the indenyl radical ($m = 115$), the fluorenyl ($m = 165$) and benzofluorenyl ($m = 215$) radicals, ethynyl indene ($m = 139$) and indenyl diethynyl ($m = 163$) can be formed by the addition of diacetylene or acetylene, respectively.

Subsequently, fluorenylacetylene ($m = 189$) and the fluorenyl-diethynyl radical ($m = 213$) were formed by successive reactions of the fluorenyl radical ($m = 165$) with acetylene.

According to Saggese *et al.*⁴², gas-phase acetylene pyrolysis reactions occur between 627 °C and 2227 °C, whereas we observe the formation of PAHs from acetylene aromatization at < 500 °C under high vacuum conditions (3×10^{-5} Torr) in the presence of SiC. Therefore, the dangling bonds of the SiC must play a crucial role in acetylene activation that reduces the energy barrier to the first aromatic ring formation.

As for the formation of chain hydrocarbons on dangling bonds of SiC, the length of the chains formed on SiC is shorter than that on alumina/pyroxene from acetylene aromatization reactions as reported by Tian *et al.*¹⁴. Only chain hydrocarbons with an even number of carbon atoms are detected. Moreover, the formation of benzo(ghi)pyrene ($m = 276$) on SiC was observed whereas on alumina/pyroxene only pyrene ($m = 202$)¹⁴ was formed from acetylene aromatization. Hence, the existence of dust grains composed of SiC is favourable for interstellar PAH formation (**Scheme 1**).

Astrophysical implications

Understanding the formation of PAHs in astrophysical environments presents significant challenges. It is widely thought that PAHs originate directly or indirectly from the chemistry of carbon-rich circumstellar envelopes (CSEs). Gas-phase neutral molecule pyrolysis and ion-molecule chemistry are considered possible routes, as

recently summarized in literature.⁴³ In our experiments using β -SiC, as well as formation of gas-phase PAHs with up to 20 carbon atoms, a soot develops which has been identified as layers of graphene. Although smaller PAHs with $N_C < 20$ can be formed *in situ* in a CSE, the surface carbon layer provides a reservoir of aromatic material which persists when the SiC grains are fully expelled into the ISM. It is notable that there is no reported detection of the characteristic 11.3 μm absorption feature of β -SiC in the ISM which may be due to oxidation²⁰ but could alternatively be due to coverage of the SiC grains by a surface layer of graphene-like material. When subjected to shocks, intense UV irradiation in photodissociation regions and cosmic rays, the surface ‘aromatic’ carbon material can be sputtered into the local ISM and so be the origin of large PAHs seen through the suite of ‘UIR’ bands. The ‘UIR’ emission bands are not expected to be seen readily from the original CSE as there is insufficient exposure to UV radiation to promote IR emission.

Acknowledgements

This work was supported by a grant from the University Research Committee of the University of Hong Kong. We thank Dr. Ming Tian for providing technical support to this work. PJS thanks the Leverhulme Trust for award of a Research Fellowship, and RG thanks the Royal Society of Chemistry for award of a Researcher Mobility Fellowship and Hong Kong University for hosting her visit.

References

- 1 A. G. G. M. Tielens, Interstellar Polycyclic Aromatic Hydrocarbon Molecules. *Annual Review of Astron. and Astrophys.* 2008, **46**, 289-337.
- 2 A. Léger, J. L. Puget, Identification of the "Unidentified IR Emission Features of Interstellar Dust". *Astron. Astrophys.* 1984, **137**, L5-L8.
- 3 M. K. Crawford, A. G. G. M. Tielens, L. J. Allamandola, Ionized Polycyclic Aromatic Hydrocarbons and Diffuse Interstellar Bands. *Astrophys. J. Part 2- Letters to the Editor* 1985, **293**, L45-L48.
- 4 H. B. Zhang, X. Q. You, C. K. Law, Role of Spin-Triplet Polycyclic Aromatic Hydrocarbons in Soot Surface Growth. *J Phys. Chem. Lett.* 2015, **6(3)**, 477-481.
- 5 R. Delaunay, M. Gatchell, P. Rousseau, A. Domaracka, S. Maclot, Y. Wang, M. H. Stockett, T. Chen, L. Adoui, M. Alcami, Molecular Growth Inside of Polycyclic Aromatic Hydrocarbon Clusters Induced by Ion Collisions. *J Phys. Chem. Lett.* 2015, **6(9)**, 1536-1542.
- 6 S. T. Ridgway, D. N. B. Hall, S. G. Kleinmann, D. A. Weinberger, R. S. Wojslaw, Circumstellar Acetylene in the IR spectrum of IRC +10° 216. *Nature* 1976, 264-345.
- 7 J. P. Fonfría, J. Cernicharo, M. J. Richter, J. H. Lacy, A Detailed Analysis of the Dust Formation Zone of IRC +10° 216 Derived from Mid-infrared Bands of C₂H₂ and HCN. *Astrophys. J.* 2008, **673**, 445-469.
- 8 I. Cherchneff, The Formation of Polycyclic Aromatic Hydrocarbons in Evolved Circumstellar Environments. *EAS Publications Series* 2011, **46**, 177-189.
- 9 M. Frenklach, E. D. Feigelson, Formation of Polycyclic Aromatic Hydrocarbons in Circumstellar Envelopes. *Astrophys. J.* 1989, **341**, 372-384.
- 10 J. A. Cole, J. D. Bittner, J. P. Longwell, J. B. Howard, Formation Mechanisms of Aromatic Compounds in Aliphatic Flames. *Combustion & Flame* 1984, 56, 51-70.

- 11 P. M. Woods, E. Herbst, The Synthesis of Benzene in the Proto-Planetary Nebula CRL 618. *Astrophys. J.* 2002, **574**, L167-L170.
- 12 F. Carelli, F. Sebastianelli, M. Satta, F. A. Gianturco, Gas-phase Route to Polycyclic Aromatic Hydrocarbon Formation in Protoplanetary Atmospheres: Role of Stabilized Benzyne Anions. *Mon. Not. R. Astron. Soc.* 2011, **415**, 425-430.
- 13 M. Tian, B. S. Liu, M. Hammonds, N. Wang, P. J. Sarre, A. S. C. Cheung, Formation of Polycyclic Aromatic Hydrocarbons from Acetylene over Nanosized Olivine-type Silicates, *Phys. Chem. Chem. Phys.* 2012, **14**, 6603-6610.
- 14 M. Tian, B. S. Liu, M. Hammonds, N. Wang, P. J. Sarre, A. S. C. Cheung, Catalytic Conversion of Acetylene to Polycyclic Aromatic Hydrocarbons (PAHs) over Particles of Pyroxene and Alumina, *Philosophical transactions. Series A, Mathematical, Phys. Eng. Sci.* 2013, **371**, 20110590.
- 15 T. Fujiyoshi, C. M. Wright, T. J. T. Moore, Mid-infrared spectroscopy of SVS13: silicates, quartz and SiC in a protoplanetary disc. *MNRAS*, 2015, **451**, 3371-3384.
- 16 A.K. Speck, G.D. Thompson, A.M. Hofmeister, Mid- and far-IR thin film (or dispersion) absorbance spectra of nanocrystalline and bulk α - and β - polytype SiC. *Astrophys. J.* 2005, **634**, 426.
- 17 P. Hoppe, 'Stardust in Meteorites and IDPs: Current Status, Recent Advances, and Future Prospects' in Cosmic Dust - Near and Far, 2009, *Astron. Soc. of Pacific Conf. Series*, **414**, 148.
- 18 A. K. Speck, A. M. Hofmeister, M. J. Barlow, The SiC Problem: Astronomical and Meteoritic Evidence. *Astrophys. J.* 1999, **513**, L87-L90.
- 19 D. Clément, H. Mutschke, R. Klein, Th. Henning, New Laboratory Spectra of Isolated β -SiC Nanoparticles: Comparison with Spectra Taken by the Infrared Space Observatory. *Astrophys. J.* 2003, **594**, 642.
- 20 D. C. B. Whittet, W. W. Duley, P. G. Martin, On the Abundance of Silicon Carbide Dust in the Interstellar Medium. *MNRAS*, 1990, 244, 427-431.
- 21 P. Merino, M. Svec, J. I. Martinez, P. Jelinek, P. Lacovig, M. Dalmiglio, S. Lizzit, P.

- Soukiassian, J. Cernicharo, J. A. Martin-Gago, Graphene Etching on SiC Grains as a Path to Interstellar Polycyclic Aromatic Hydrocarbons Formation. *Nature commun.* 2014, **5**, 3054.
- 22 M. Bhatnagar, B. J. Baliga, Comparison of 6H-SiC, 3C-SiC and Si for Power Devices. *IEEE Transactions on Electron Devices* 1993, **40**, 645-655.
- 23 M. A. Vannice, Y. L. Chao, R. M. Friedman, The Preparation and Use of High Surface Area Silicon Carbide Catalyst Supports. *Appl. Catal.* 1986, **20**, 91-107.
- 24 W. Z. Sun, G. Q. Jin, X. Y. Guo, Partial Oxidation of Methane to Syngas over Ni/SiC Catalysts. *Catal. Commun.* 2005, **6**, 135.
- 25 T. L. Church, S. Fallani, J. Liu, M. Zhao, A. T. Harris, Novel Biomorphic Ni/SiC Catalysts that Enhance Cellulose Conversion to Hydrogen. *Catal. Today* 2012, **190**, 98.
- 26 H. Ba, Y. Liu, X. Mu, W-H. Doh, J. Nhut, P. Granger, C. Pham-Huu, Macroscopic nanodiamonds/ β -SiC composite as metal-free catalysts for steam-free dehydrogenation of ethylbenzene to styrene. *Appl. Catal. A* 2015, **499**, 217-226.
- 27 E. M. McCash, In *Surface Chemistry*; Oxford University Press Inc: New York, 2001, p40.
- 28 Y. Baron, R. Papoular, M. Jourdain de Muizon, B. Pégourié, An Analysis of the Emission Features of the IRAS Low-Resolution Spectra of Carbon Stars. *Astron. Astrophys.* 1987, **186**, 271-279.
- 29 W. G. Spitzer, D. Kleinman, D. Walsh, Infrared Properties of Hexagonal Silicon Carbide *Phys. Review* 1959, **113**, 127.
- 30 B. Shukla, M. Koshi, A Highly Efficient Growth Mechanism of Polycyclic Aromatic Hydrocarbons. *Phys. Chem. Chem. Phys.* 2010, **12**, 2427-37.
- 31 Y. H. Guo, C. Xia, B. S. Liu, Catalytic Properties and Stability of Cubic Mesoporous $\text{La}_x\text{Ni}_y\text{O}_z/\text{KIT-6}$ Catalysts for CO_2 Reforming of CH_4 . *Chem. Eng. J.*

- 2014, **237**, 421–429.
- 32 B. S. Liu, L. Jiang, H. Sun, C. T. Au, XPS, XAES, and TG/DTA Characterization of Deposited Carbon in Methane Dehydroaromatization over Ga–Mo/ZSM-5 Catalyst. *Appl. Surf. Sci.* 2007, **253**, 5092-5100.
- 33 P. G. Soukiassian, H. B. Enriquez, Atomic Scale Control and Understanding of Cubic Silicon Carbide Surface Reconstructions, Nanostructures and Nanochemistry. *J. Phys.:Condensed Matter* 2004, **16**, S1611-S1658.
- 34 J. F. Li, C. Xia, C. T. Au, B. S. Liu, Y₂O₃-Promoted NiO/SBA-15 Catalysts Highly Active for CO₂/CH₄ Reforming, *Intern. J. Hydrogen Energy* 2014, **39**, 10927.
- 35 J. Leifeld, Thermal Stability of Black Carbon Characterized by Oxidative Differential Scanning Calorimetry. *Organic Geochem.* 2007, **38**, 112-127.
- 36 J.P. Perdew, Y. Wang, Accurate and Simple Analytic Representation of the Electron-gas Correlation Energy. *Phys. Rev. B* 1992, **45**, 13244.
- 37 J. Wieferink, P. Krüger, J. Pollmann, First-principles Study of Acetylene Adsorption on β -SiC(001)-(3 \times 2). *Phys Rev. B* 2007, **75**, 153305-1.
- 38 A.J. Dyson, P. V. Smith, Empirical Potential Study of the Chemisorption of C₂H₂ and CH₃ on the β -SiC(001) Surface. *Surf. Sci.* 1998, **396**, 24-39.
- 39 H. Sabbah, L. Biennier, S.J. Klippenstein, I.R. Sims, B.R. Rowe, Exploring the Role of PAHs in the Formation of Soot: Pyrene Dimerization. *J. Phys. Chem. Lett.* 2010, **1**(19), 2962-2967.
- 40 V. V. Kislov, A. I. Sadovnikov, A. M. Mebel, Formation Mechanism of Polycyclic Aromatic Hydrocarbons Beyond the Second Aromatic Ring. *J. Phys. Chem. A* 2013, **117**, 4794-816.
- 41 F. T. Zhang, R. I. Kaiser, V. V. Kislov, A. M. Mebel, A. Golan, M. Ahmed, A VUV Photoionization Study of the Formation of the Indene Molecule and Its Isomers. *J. Phys. Chem. Lett.* 2011, **2** (14), 1731-1735.
- 42 C. Saggese, N. E. Sánchez, A. Frassoldati, A. Cuoci, T. Faravelli, M. U. Alzueta, E.

- Ranzi, Kinetic Modeling Study of Polycyclic Aromatic Hydrocarbons and Soot Formation in Acetylene Pyrolysis. *Energy Fuels* 2014, **28**, 1489-1501.
- 43 R. I. Kaiser, D. S. N. Parker, A. M. Mebel, Reaction Dynamics in Astrochemistry: Low-Temperature Pathways to Polycyclic Aromatic Hydrocarbons in the Interstellar Medium. *Annu. Rev. Phys. Chem.* 2015, **66**:43–67.

Table Legend and Scheme:

Scheme 1. Map of proposed mechanisms for acetylene aromatization reactions.

Table 1. PAH Groups detected Based on Mass Interval

Figure captions:

Figure 1. Schematic of TOF-MS apparatus for catalytic conversion reaction of acetylene to PAHs over SiC.

Figure 2. HRTEM images, SAED (inset), (c) XRD patterns and (d) FT-IR spectra over (a) α -SiC and (b) β -SiC.

Figure 3. TOF-MS signals from acetylene conversion over β -SiC as a function of temperature in the mass range (a) 0 – 80 and (b) 75 – 275.

Figure 4. GC signals of solution obtained from the surface of β -SiC (solution A) and from the cold-trap (solution B). Peaks are annotated with the mass number of the base peak from the corresponding mass spectrum.

Figure 5. Comparison of PAH formation on β -SiC and α -SiC at different temperatures. The numerical values are the molecular weight of the PAHs formed.

Figure 6. TG/DTG profiles and HRTEM images over used (a, c) α -SiC and (b, d) β -SiC at 550 °C (red), 650 °C (green) and 750 °C (blue), respectively after TOF-MS reactions.

Figure 7. TOF-MS signals of the catalytic conversion of different hydrocarbons on β -SiC at 600 °C.

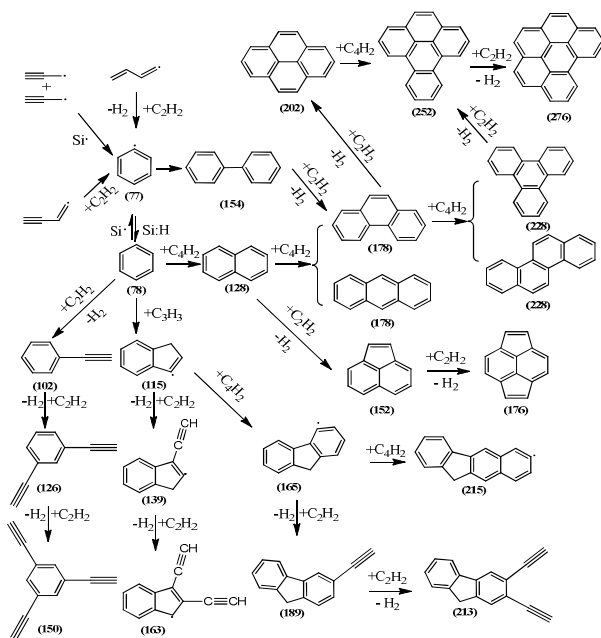
Scheme 1. Map of proposed mechanisms for acetylene aromatization reactions.

Table 1. PAH Groups detected Based on Mass Interval

Sequence No. (mass interval)	Mass	Formula	Name	TOF- MS	GC- MS
1(24)	78	C ₆ H ₆	Benzene	●	○
	102	C ₈ H ₆	Phenylacetylene	●	○
	126	C ₁₀ H ₆	1,3-diethylbenzene	●	○
	150	C ₁₂ H ₆	1,3,5-triethynylbenzene	●	○
2(50)	78	C ₆ H ₆	Benzene	●	○
	128	C ₁₀ H ₈	Naphthalene	●	●
	178	C ₁₄ H ₁₀	Anthracene /phenanthrene	●	●
	228	C ₁₈ H ₁₂	Chrysene /triphenylene	●	●
3(24)	128	C ₁₀ H ₈	Naphthalene	●	●
	152	C ₁₂ H ₈	Acenaphthylene	●	●
	176	C ₁₄ H ₈	Pyracylene	●	○
4(24)	115	C ₉ H ₇	Indenyl radical	●	●*
	139	C ₁₁ H ₇	Ethynyl indene	●	○
	163	C ₁₃ H ₇	Indenyldiethynyl	●	○
5(50)	115	C ₉ H ₇	Indenyl radical	●	●*
	165	C ₁₃ H ₉	Fluorenyl radical	●	●**
	215	C ₁₇ H ₁₁	Benzofluorenyl	●	●***
6(24)	165	C ₁₃ H ₉	Fluorenyl radical	●	●**
	189	C ₁₅ H ₉	Fluorenylacetylene	●	●
	213	C ₁₇ H ₉	Fluorenyldiethynyl	●	○
7(24)	74	C ₆ H ₂	Triacetylene	●	○
	98	C ₈ H ₂	Tetraacetylene	●	○
	122	C ₁₀ H ₂	Pentaacetylene	●	○
8(24)	154	C ₁₂ H ₁₀	Biphenyl	○	●
	178	C ₁₄ H ₁₀	Anthracene /phenanthrene	●	●
	202	C ₁₆ H ₁₀	Pyrene	●	●
9(50)	142	C ₁₁ H ₁₀	1(2)-methylnaphthalene	●	●
	192	C ₁₅ H ₁₂	Methylphenanthrene / methylantracene	●	●
10(24)	228	C ₁₈ H ₁₂	Chrysene†	●	●
	252	C ₂₀ H ₁₂	Benzo(e)pyrene†	●	●
	276	C ₂₂ H ₁₂	Benzo(ghi)pyrene†	○	●

Notes: (a) owing to their instability, radicals were not detected directly by GC-MS. Rather, they were observed in their corresponding stable forms, i.e. hydrogenated molecules. *:116; **:166; ***:216; (b) for the higher mass PAHs, assignments marked with a † indicate that there exists more than one stable isomeric form.

Figure 1. Schematic of TOF-MS apparatus for catalytic conversion reaction of acetylene to PAHs over SiC.

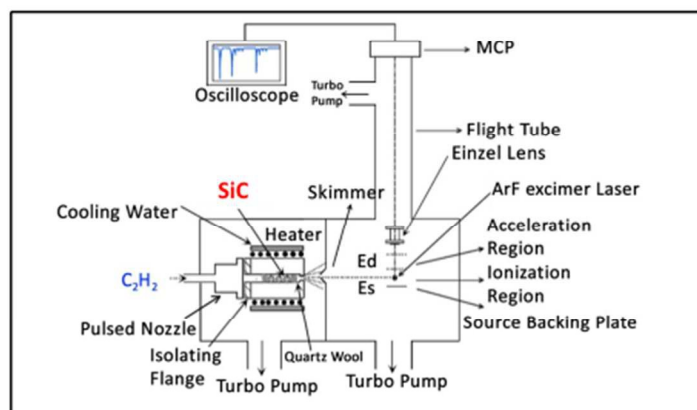


Figure 2. HRTEM images, SAED (inset), (c) XRD patterns and (d) FT-IR spectra over (a) α -SiC and (b) β -SiC.

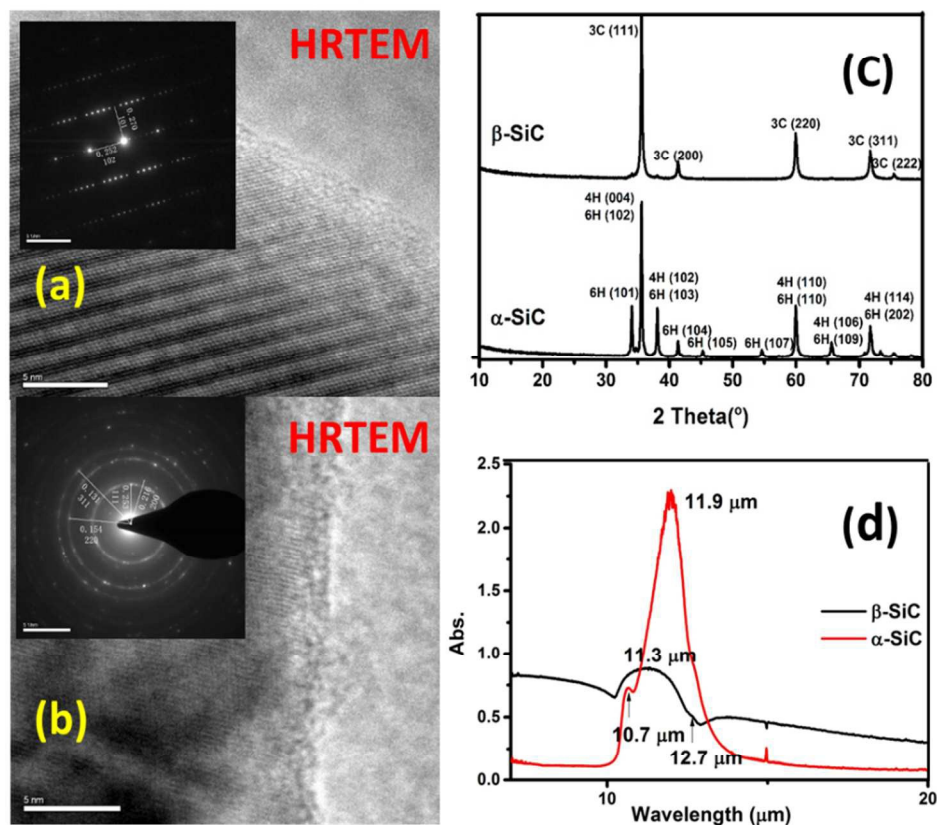


Figure 3. TOF-MS signals from acetylene conversion over β -SiC as a function of temperature in the mass range (a) 0 – 80 and (b) 75 - 275

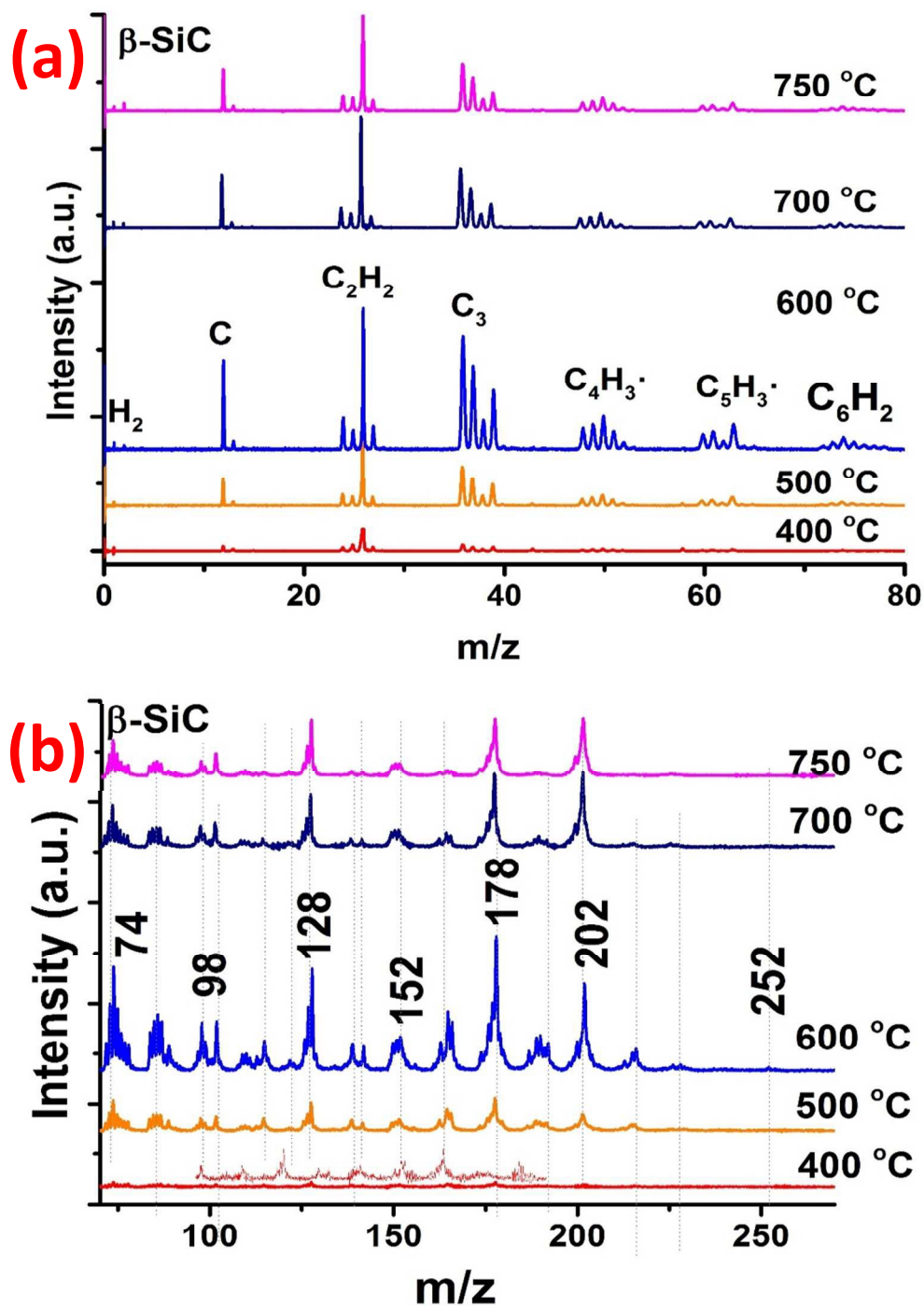


Figure 4. GC signals of solution obtained from the surface of β -SiC (solution A) and from the cold-trap (solution B). Peaks are annotated with the mass number of the base peak from the corresponding mass spectrum.

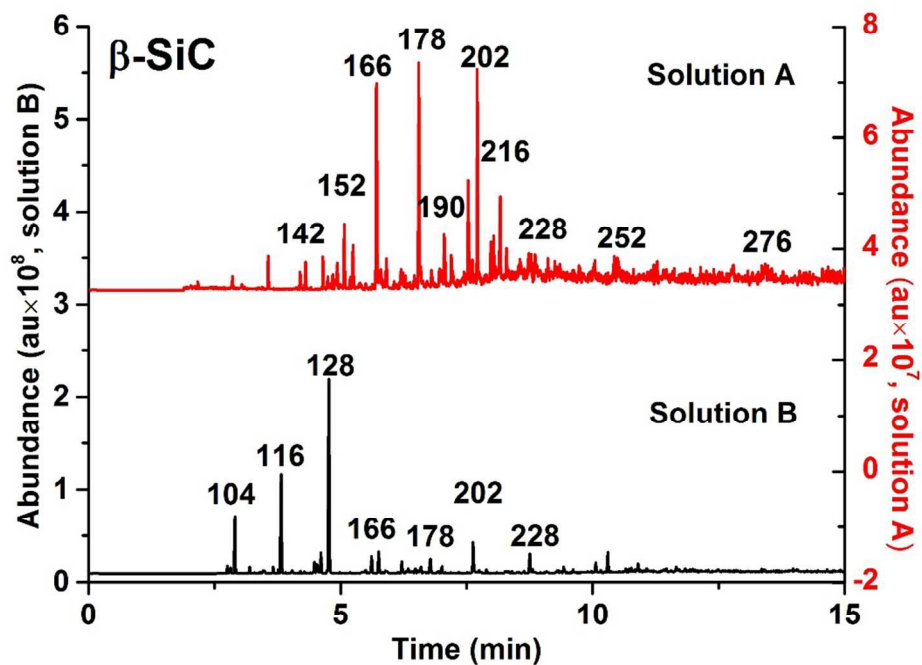


Figure 5. Comparison of PAH formation on β -SiC and α -SiC at different temperatures. The numerical values are the molecular weight of the PAHs formed.

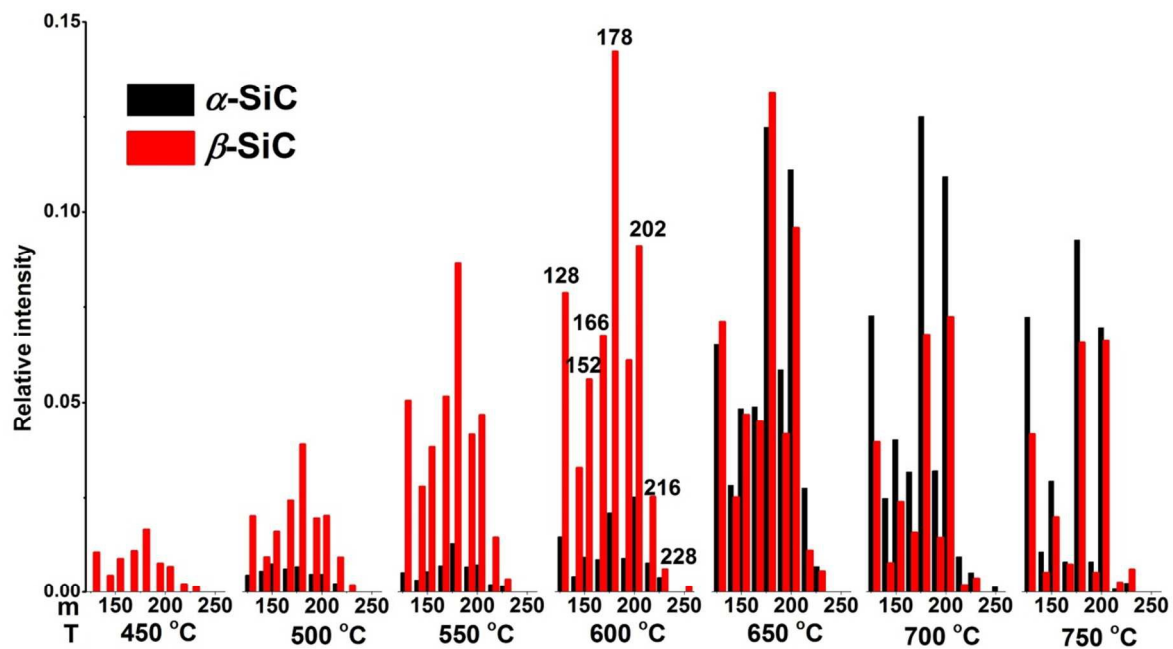


Figure 6. TG/DTG profiles and HRTEM images over used (a, c) α -SiC and (b, d) β -SiC at 550 °C (red), 650 °C (green) and 750 °C (blue), respectively after TOF-MS reactions.

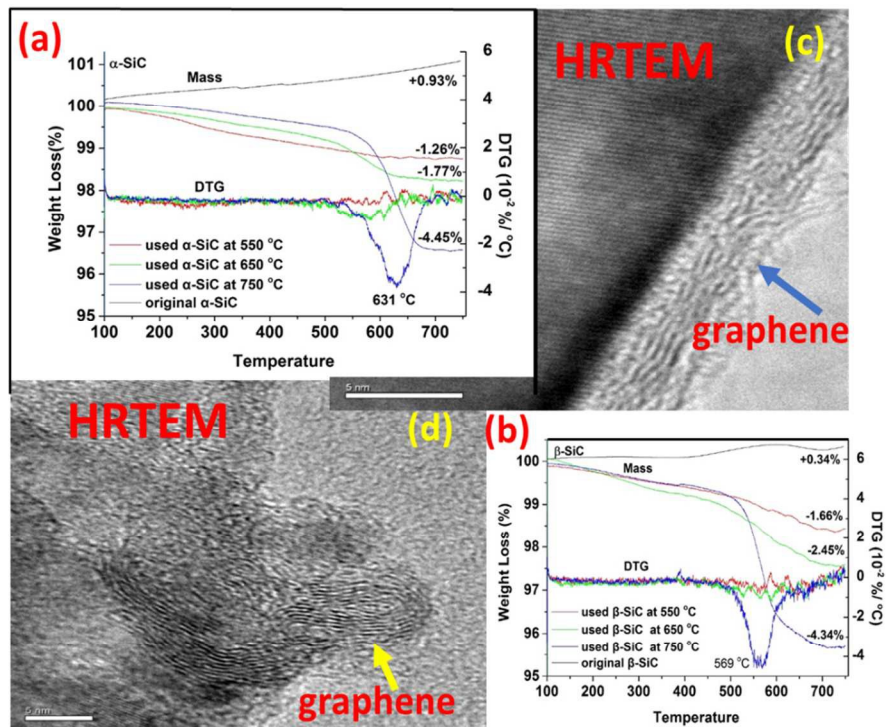


Figure 7. TOF-MS signals of the catalytic conversion of different hydrocarbons on β -SiC at 600 $^{\circ}$ C.

